

Supplementary Information for

Directly Printed Wearable Electronic Sensing Textiles towards Human-Machine Interfaces

*Xinqin Liao,^a Weitao Song,^{a,b} Xiangyu Zhang,^a Hua Huang,^c Yongtian Wang,^{b,d} and
Yuanjin Zheng^a*

- a.* School of Electrical and Electronic Engineering, Nanyang Technological University, 50 Nanyang Avenue, Singapore 639798, Singapore.
- b.* AICFVE of Beijing Film Academy, 4 Xitucheng Road, Beijing 100088, China.
- c.* Beijing Key Lab of Intelligent Information Technology, School of Computer Science, Beijing Institute of Technology, 5 Zhongguancun South Street, Beijing 100081, China.
- d.* Beijing Engineering Research Centre of Mixed Reality and Advanced Display, School of Optics and Photonics, Beijing Institute of Technology, 5 Zhongguancun South Street, Beijing 100081, China.

Supplementary materials

Fig. S1. Schematic illustration of the fabricating process of the textile strain sensor.

Fig. S2. SEM image and corresponding EDS mapping image of the textile strain sensor partially printed with silver ink.

Fig. S3. Cross-sectional SEM image and corresponding EDS mapping image of the textile strain sensor.

Fig. S4. Current-voltage (I - V) characteristic curves of the textile strain sensor stretched by 0% and 5% strain.

Fig. S5. Variation in the normalized resistance of the counterpart device prepared without pre-stretching action under different strain.

Fig. S6. Flow chart of the textile strain sensors as a smart car director.

Fig. S7. Diagram of the intelligent glove assembled with five textile strain sensors as a smart car director.

Fig. S8. Flow chart of the integrated textile strain sensors for wireless typing.

Fig. S9. Diagram of the intelligent glove assembled with five printed textile strain

sensors for wireless typing.

Fig. S10. Flow chart of the textile strain sensors for remotely controlling PowerPoint slides.

Fig. S11. Diagram of the intelligent glove assembled with five textile strain sensors as remote PowerPoint controller.

Table S1. Comparison of textile- or fiber-based strain sensors in the aspects of fabrication method, sensing range, and sensitivity.

Video S1. Demonstrator 1: the textile strain sensors as a smart car director.

Video S2. Demonstrator 2: the textile strain sensors used for wireless typing.

Video S3. Demonstrator 3: the textile strain sensors as a remote PowerPoint controller.

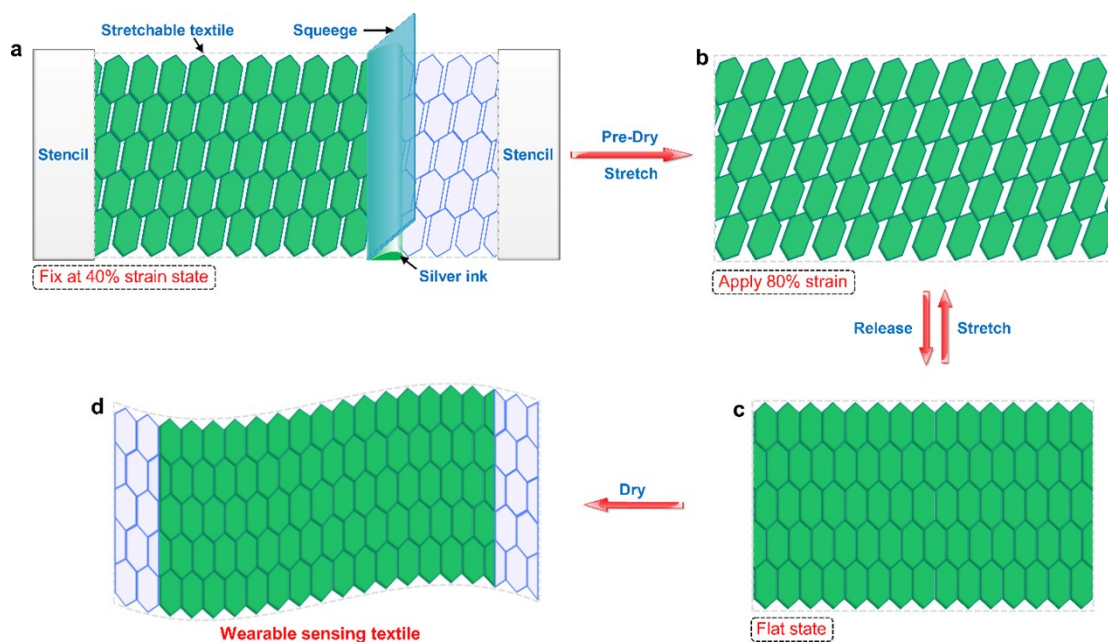


Fig. S1. (a-d) Schematic illustration of the fabricating process of the textile strain sensor.

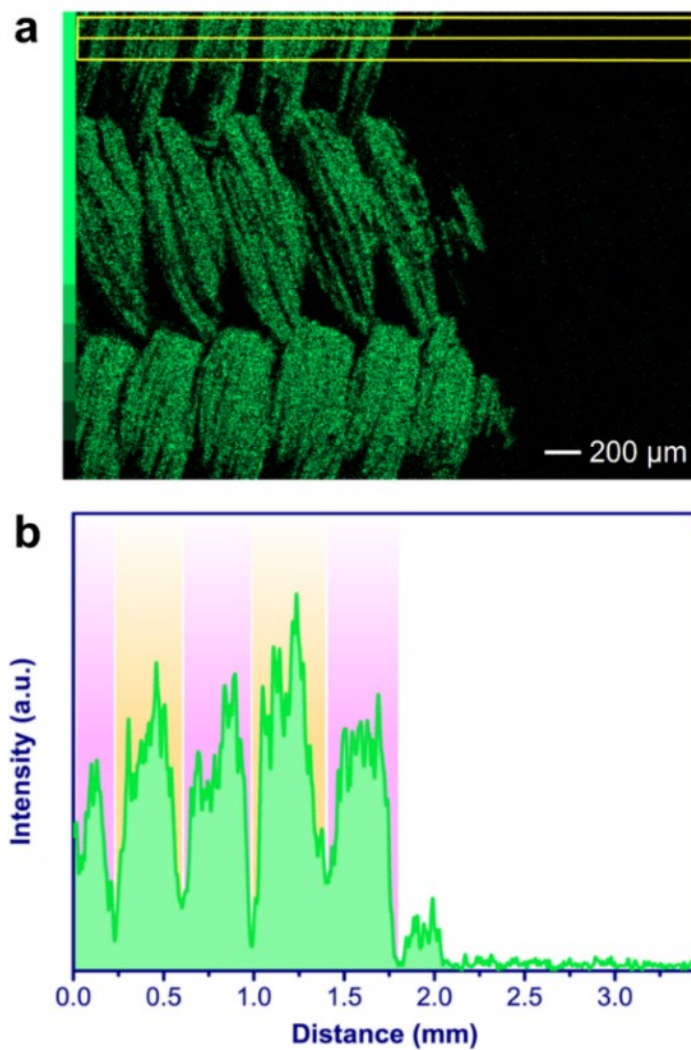


Fig. S2. (a) Surface distribution of the silver element image of the textile partially printed with silver ink. The green patterned image was the distribution of the silver element. (b) Energy intensity of the silver element in the yellow wireframe area of (a). The five mountain peaks, which reflected the high intensity of the silver element, indicating the five clusters of polyester in the yellow wireframe area of (a).

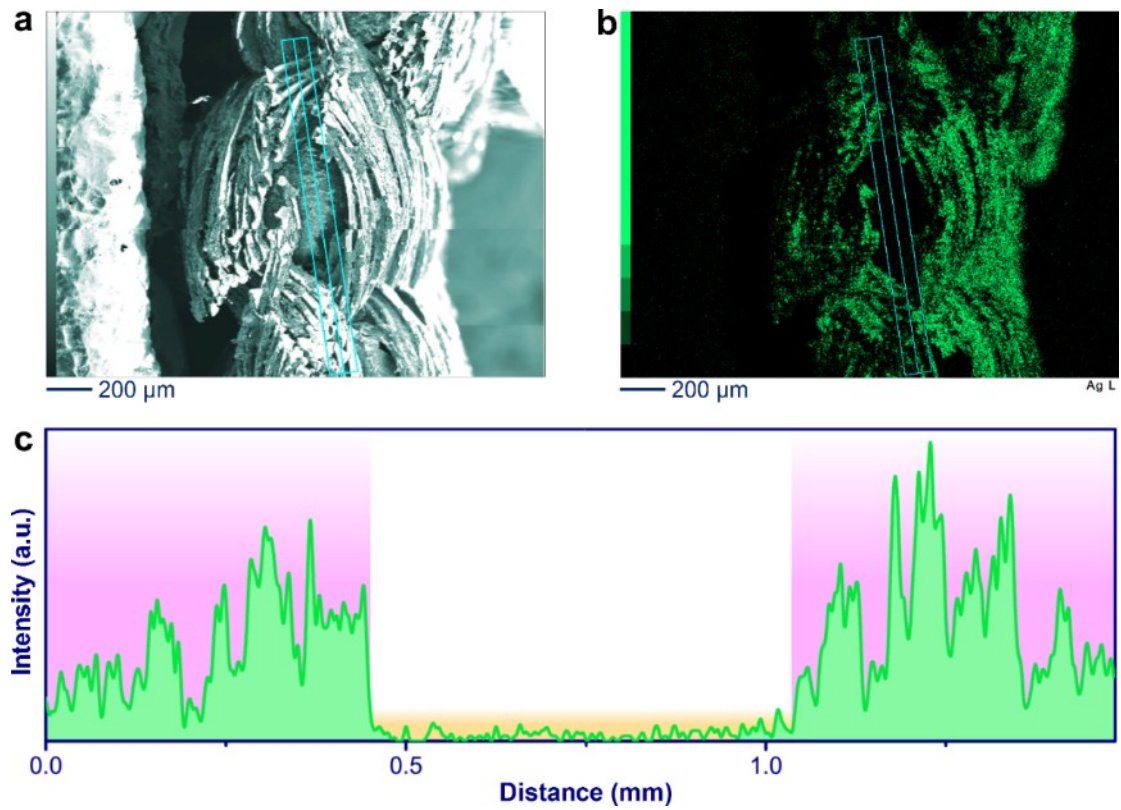


Fig. S3. (a, b) Cross-sectional SEM image, and corresponding EDS mapping image of the textile strain sensor. The surface distribution of the silver element was clearly observed from the green patterned image. (c) Energy intensity of the silver element in the light blue wireframe area of (b). The low intensity part indicated the elastic latex thread, which was the core fiber of the textile.

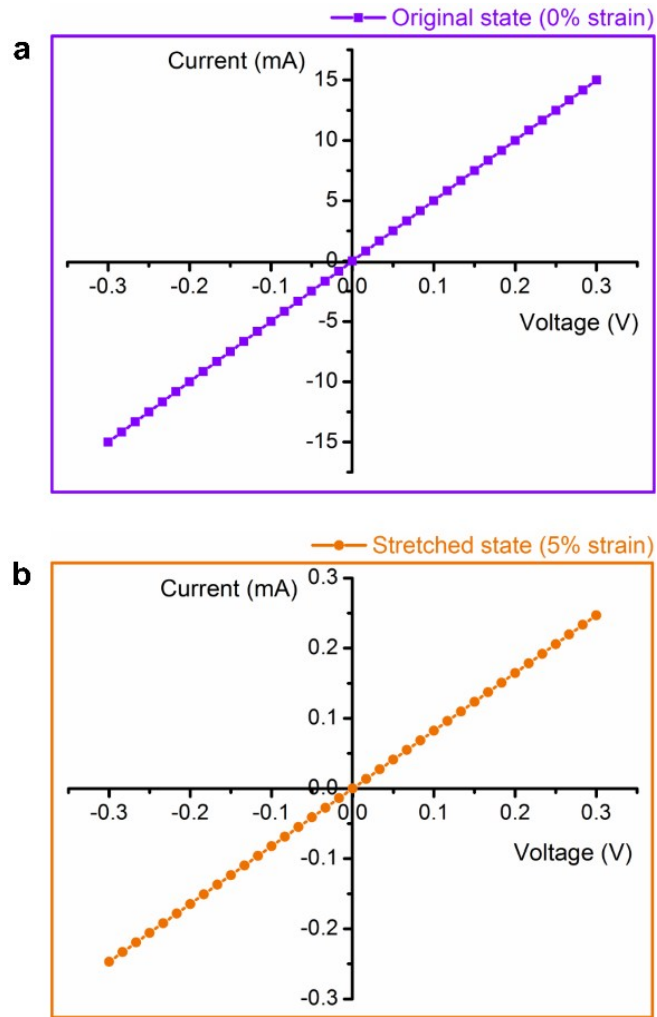


Fig. S4. (a-b) Current-voltage (I - V) characteristic curves of the textile strain sensor stretched by 0% and 5% strain. It could be found that the current of the textile strain sensor was changed at the same voltage when the external strain was applied. Nevertheless, no matter being subjected to external strain or not, both characteristic curves were linear, implying ohmic characteristic of the textile strain sensor. Thus, the textile strain sensor belonged to resistive strain-sensing device.

Table S1. Comparison of textile- or fiber-based strain sensors in the aspects of fabrication method, sensing range, and sensitivity.

Materials	Fabrication method	Sensing range^(a)	Gauge factor^(b)	Reference
Carbon nanotube /Spandex	Knitting	~80%	0.4	(S1)
Poly(3,4-ethylenedioxythiophene)/Polyester	Polymerization	20%	1	(S2)
Poly(3,4-ethylenedioxythiophene):poly(styrene sulfonate)/Polyurethane fibers	Spinning and knitting	160%	~1	(S3)
Piezoresistive rubber/Silver nanowires/Nylon	Surface-modifying, dip-coating, and weaving	20%	2.75	(S4)
Graphite flakes/Silk fibers	Dry-Meyer-rod-coating	15%	14.5	(S5)
ZnO nanowires/Polyurethane fibers	Soak-coating and hydrothermal reaction	10%	15.2	(S6)
Carbon thread/Polydimethylsiloxane	Carbonization and dip-coating	8-10%	18.5	(S7)
Reduced graphene oxide/Nylon/Polyurethane	Soak-coating and hydroiodic reduction	0-10%	18.5	(S8)
ZnO nanowires/Carbon fiber	Dip-coating and hydrothermal reaction	1.2%	~45	(S9)
Cotton fabric	Carbonization	80%-140%	64	(S10)
Graphite flakes/Human hairs	Dry-Meyer-rod-coating	~10%	71.1	(S5)
Silver microflakes/Polyester filaments/Elastic latex threads	Stencil printing	60%	~2,000	This work

Note: (a) This sensing range referred to the detection range when the GF attained its maximum value. (b) Here GF was the maximum value of the corresponding sensor.

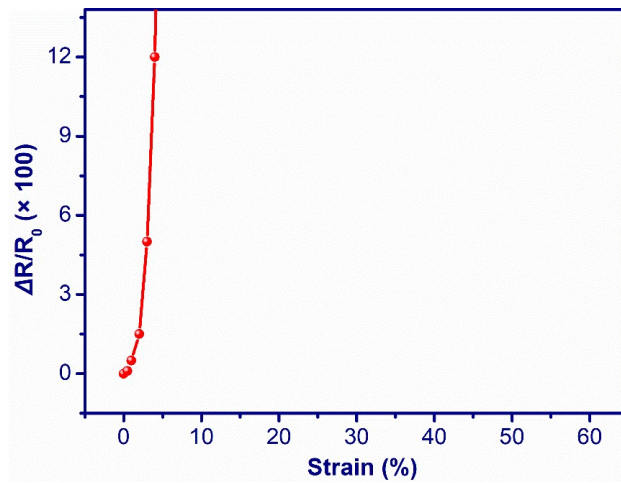


Fig. S5. Variation in the normalized resistance of the counterpart device prepared without pre-stretching action under different strain.

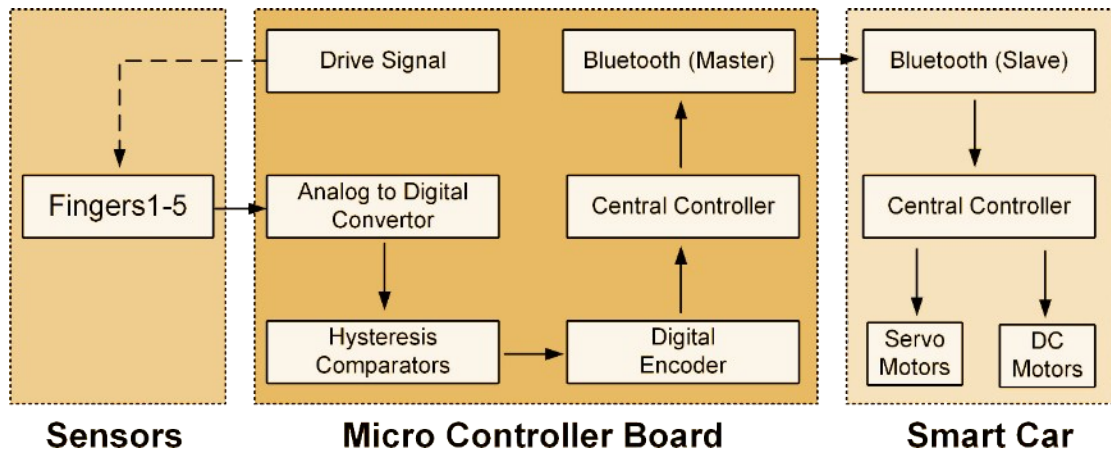


Fig. S6. Flow chart of the textile strain sensors as a smart car director.

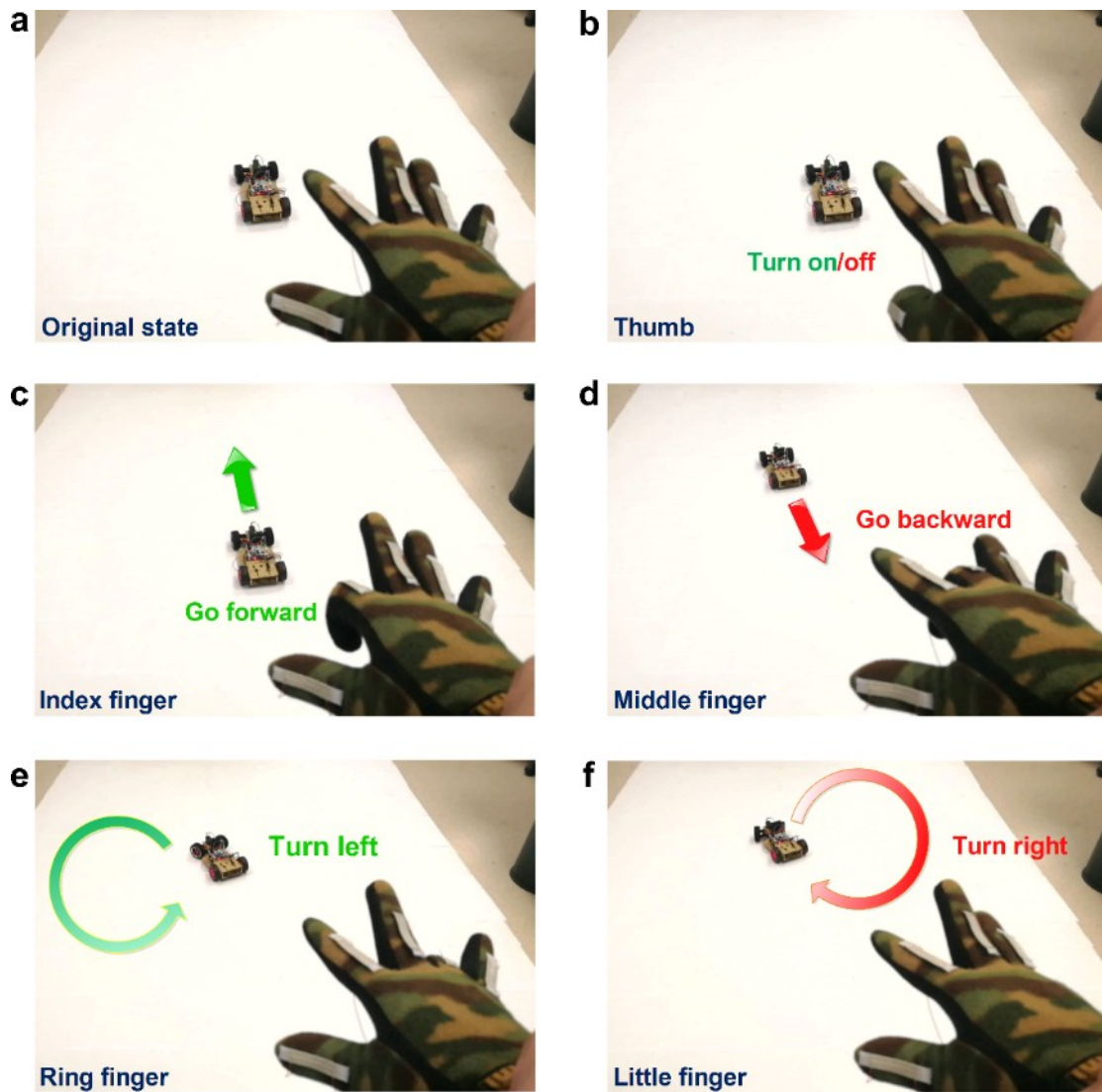


Fig. S7. (a-f) Diagram of the intelligent glove assembled with five printed textile strain sensors as a smart car director. The functional commands of “Turn on/off”, “Go forward”, “Go backward”, “Turn left”, and “Turn right” were respectively issued by the thumb, index fingers, middle finger, ring finger, and little finger.

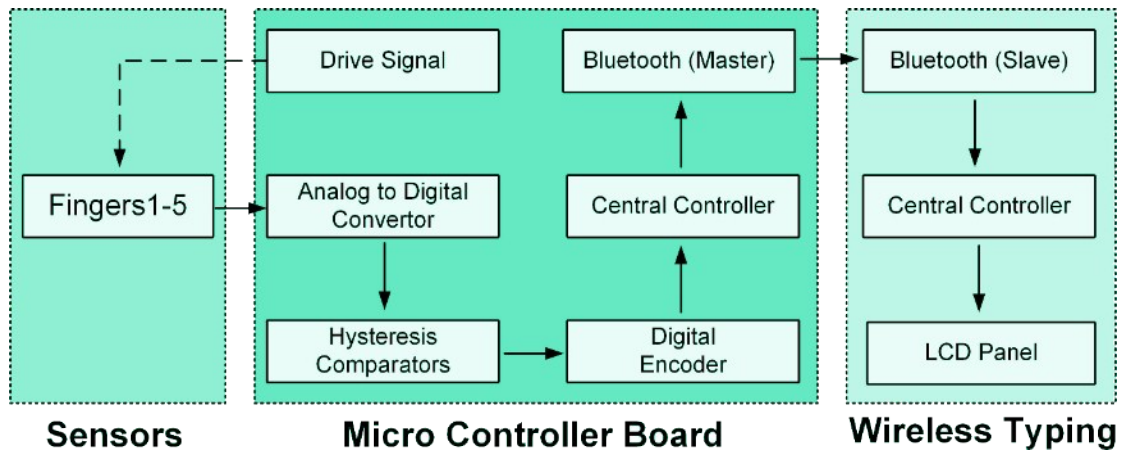


Fig. S8. Flow chart of the textile strain sensors for wireless typing.

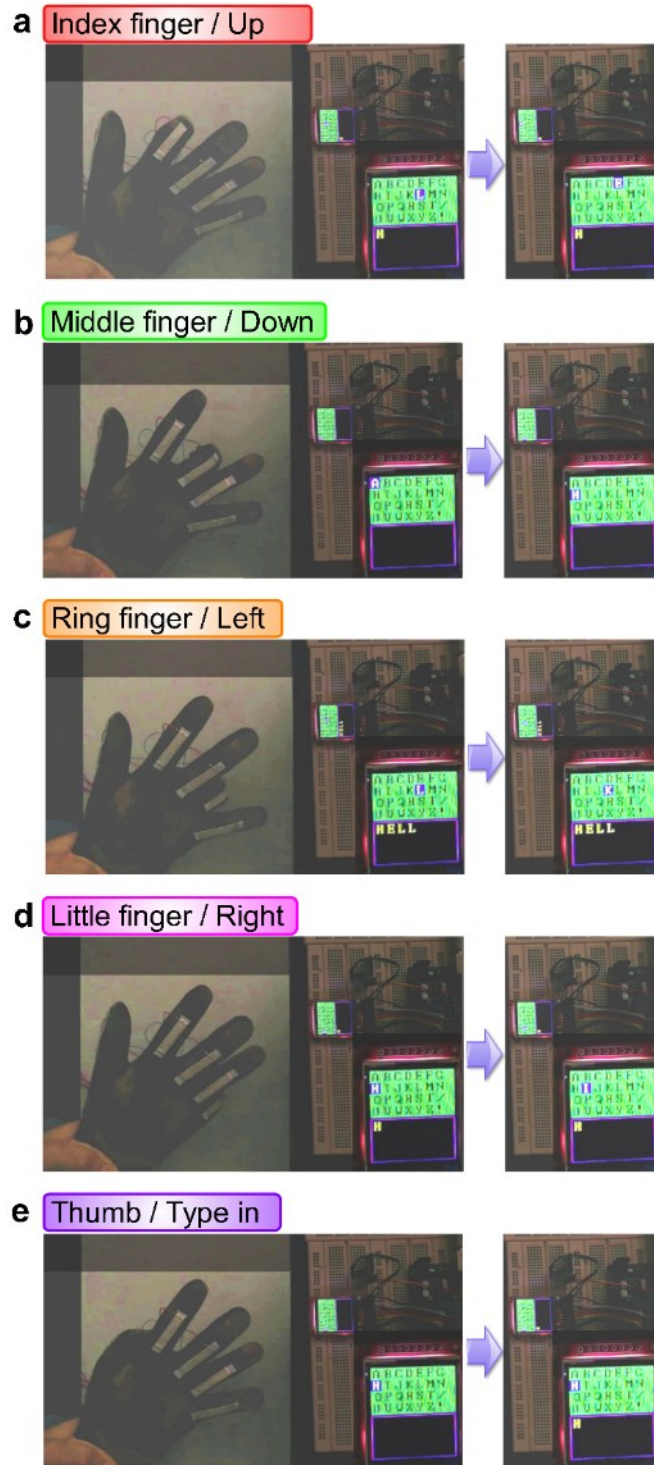


Fig. S9. (a-e) Diagram of the intelligent glove assembled with five textile strain sensors for wireless typing. The functional commands of “Type in”, “Turn up”, “Turn down”, “Turn left”, and “Turn right” were respectively issued by the thumb, index fingers, middle finger, ring finger, and litter finger.

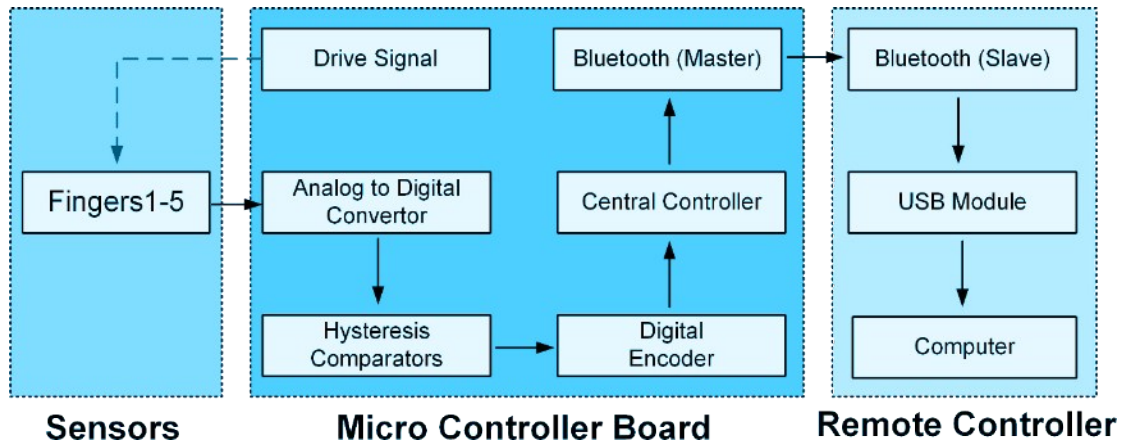


Fig. S10. Flow chart of the textile strain sensors for remotely controlling PowerPoint slides.

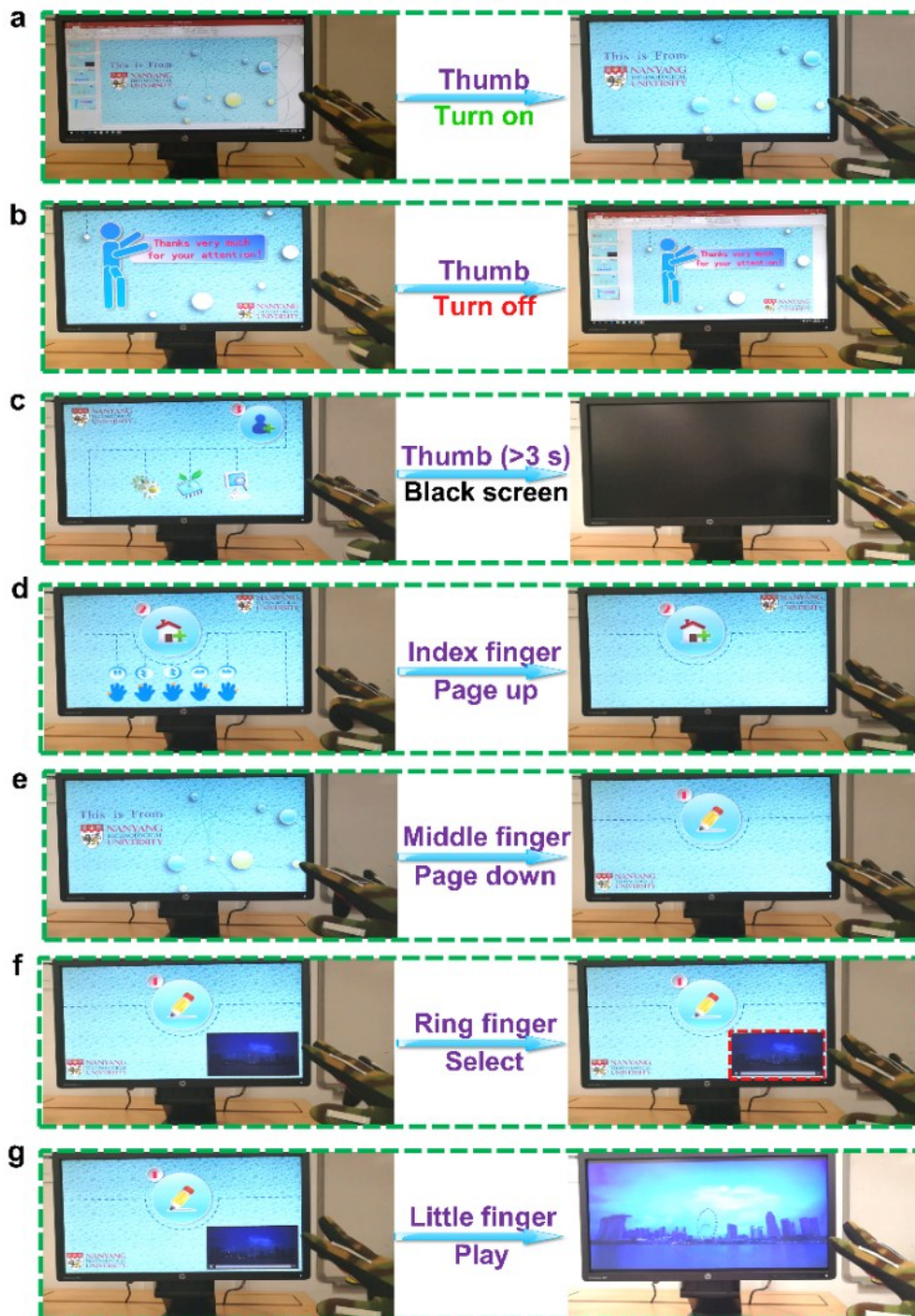


Fig. S11. (a-g) Diagram of the intelligent glove assembled with five printed textile strain sensors as a remote PowerPoint controller. The short bending of thumb indicated the functional commands of “Turn on” and “Turn off”. The long bending (>3 s) of thumb made the screen black. The other functional commands of “Page Up” and “Page down” were respectively controlled by the index fingers and middle finger. The ring finger and little finger respectively issued the functional commands of “Select hyperlink” and “Play video”.

Supplementary references

- S1 J. Foroughi, G. M. Spinks, S. Aziz, A. Mirabedini, A. Jeiranikhameneh, G. G. Wallace, M. E. Kozlov and R. H. Baughman, *ACS Nano*, 2016, **10**, 9129.
- S2 J. Eom, R. Jaisutti, H. Lee, W. Lee, J. S. Heo, J. Y. Lee, S. K. Park and Y. H. Kim, *ACS Appl. Mater. Interfaces*, 2017, **9**, 10190.
- S3 S. Seyedin, J. M. Razal, P. C. Innis, A. Jeiranikhameneh, S. Beirne and G. G. Wallace, *ACS Appl. Mater. Interfaces*, 2015, **7**, 21150.
- S4 J. Ge, L. Sun, F. R. Zhang, Y. Zhang, L. A. Shi, H. Y. Zhao, H. W. Zhu, H. L. Jiang and S. H. Yu, *Adv. Mater.*, 2016, **28**, 728.
- S5 M. Zhang, C. Wang, Q. Wang, M. Jian and Y. Zhang, *ACS Appl. Mater. Interfaces*, 2016, **8**, 20894.
- S6 X. Liao, Q. Liao, Z. Zhang, X. Yan, Q. Liang, Q. Wang, M. Li and Y. Zhang, *Adv. Funct. Mater.*, 2016, **26**, 3074.
- S7 Y. Q. Li, P. Huang, W. B. Zhu, S. Y. Fu, N. Hu and K. Liao, *Sci. Rep.*, 2017, **7**, 45013.
- S8 G. Cai, M. Yang, Z. Xu, J. Liu, B. Tang and X. Wang, *Chem. Eng. J.*, 2017, **325**, 396.
- S9 Q. Liao, M. Mohr, X. Zhang, Z. Zhang, Y. Zhang and H. J. Fecht, *Nanoscale*, 2013, **5**, 12350.
- S10 M. Zhang, C. Wang, H. Wang, M. Jian, X. Hao and Y. Zhang, *Adv. Funct. Mater.*, 2017, **27**, 1604795.